Journal of Systems Engineering and Electronics
Vol. 35, No. 4, August 2024, pp.1053 – 1062

Quantitative method for calculating spatial release region for laser-guided bomb

YANG Ping[1,*], XIAO Bing[1], CHEN Xin[1], and HAO Yuntao[2]

1. Air Force Early Warning Academy, Wuhan 430019, China; 2. Unit 93175 of the PLA, Changchun 136000, China

Abstract: The laser-guided bomb (LGB) is an air-to-ground precision-guided weapon that offers high hit rates, great power, and ease of use. LGBs are guided by semi-active laser ground-seeking technology, which means that atmospheric conditions can affect their accuracy. The spatial release region (SRR) of LGBs is difficult to calculate precisely, especially when there is a poor field of view. This can result in a lower real hit probability. To increase the hit probability of LGBs in tough atmospheric situations, a novel method for calculating the SRR has been proposed. This method is based on the transmittance model of the 1.06 μm laser in atmospheric species and the laser diffuse reflection model of the target surface to determine the capture target time of the laser seeker. Then, it calculates the boundary ballistic space starting position by ballistic model and gets the spatial scope of the spatial release region. This method can determine the release region of LGBs based on flight test data such as instantaneous velocity, altitude, off-axis angle, and atmospheric visibility. By more effectively employing aircraft release conditions, atmospheric visibility and other factors, the SRR calculation method can improve LGB hit probability by 9.2%.

Keywords: laser-guided bombs (LGBs), hit probability, atmospheric transmittance, spatial release region (SRR) boundary ballistic.

DOI: 10.23919/JSEE.2024.000083

1. Introduction

Laser-guided bombs (LGBs) are guided by semi-active laser ground-seeking technology, which requires the laser designation pod (LDP) to illuminate the target constantly until the bomb strikes its mark. In general, LGBs can only hit stationary and slow-moving targets with velocities below 25 km/h. The attack mechanism consists of a self-designation attack and a cooperative attack [1]. In actual LGB use, the optimal release region must be calculated to optimize hit probability and destructive effect. Many factors can affect the scope of LGB's spatial release region (SRR). The LGB guidance system is relatively straightforward, with guidance errors constituting a minor portion of the error cause. In contrast, unguided errors such as initial launch status, ballistic design, atmospheric parameters, geographic environment [2], and human operational errors are the main sources of error. Laser guidance signal propagation in the atmosphere, attenuation, target diffuse reflection and other processes help reach the laser seeker so that LGBs can be guided to their targets. Therefore, atmospheric parameters have a crucial influence on LGB's hitting ability. Consequently, it is significant to precisely determine the optimal SRR of LGBs in poorer atmospheric conditions.

To improve the probability of hitting a target with LGBs, some scholars have proposed a SRR numerical model. These studies are based on ballistic models and use specific guidance law algorithms to ensure weapon hit rates and terminal miss distance. Currently, the majority of guided bombs employ proportional guidance, which satisfies weapon criteria for circular error probable (CEP) [3−5]. Determining the LGB release region is crucial for increasing hit probability and decreasing CEP. Huang et al. and Chen et al. proposed a mathematical model for the continuous computational release region (CCRR) [6,7]. And [8,9] applied the CCRR attack method to LGB semi-physical simulation tests and investigated accuracy aspects. The CCRR attack method does not take into account the variation in received irradiance within the field of view of the laser seeker, nor does it examine the calculation error of the final result with the source of error. Therefore, the optical guidance path (OGP) needs to be studied and analyzed. Finding the boundary ballistics that satisfy the guidance law by laser seeker receiving energy change is an effective way to determine SRR.

Manuscript received March 13, 2023.
*Corresponding author.
This work was supported by the major research projects within the military-international class (JY2021B077).

To obtain the energy change received by the laser seeker during the aiming process, we need to study the propagation of laser light in the atmosphere. The Mie scattering theory is usually applied in engineering to approximate the attenuation of laser energy by aerosols in the atmosphere [10−12]. The effect of atmospheric aerosols on the attenuation of laser transmission in visible and near-infrared wavelengths was discussed and analyzed. References [13,14] gave aerosols' composition and seasonal trends in different regions, including desert, Gobi, and ocean. Atmospheric radiant energy calculation aids were used by [15,16] to quantify illumination paths, angle of incidence, altitude, and atmospheric transmittance for a variety of atmospheric conditions. References [17,18] investigated the physical process of obtaining diffuse reflection signals and studied the spatial distribution of laser reflection signals at two wavelengths, 1.06 μm and 10.6 μm, respectively.

The comprehensive analysis examines the ballistic model, the laser transmission model in the atmosphere, and the diffuse reflection model of the target. The energy changes received by the laser seeker during the strike process are simulated. The boundary ballistics capable of accurately hitting the target are determined through constraints such as the laser seeker's capture moment, field of view angle, and guidance law. Through simulation calculations, a set of initial release point spatial locations for all boundary ballistics is obtained. The set of all eligible points is the SRR of the LGB. Using this calculation method, the SRR of the aircraft can be determined more accurately based on the launch parameters and atmospheric conditions of the aircraft.

2. Definition of SRR

Given the low atmospheric visibility and unknown terrain in the mission area, the window of opportunity for an attack is limited. To increase the likelihood of a successful strike, the aircraft must approach the target and use a self-designated attack. This necessitates consistent illumination of the target by the aircraft's LDP until impact.

The laser seeker of the LGB must receive sufficient diffuse energy density from the target within its field of view. However, the laser transmittance in the atmosphere is affected by multiple factors such as propagation distance, angle, and visibility. Therefore, the SRR of the LGB must be limited to a specific spatial region to ensure successful target acquisition, as shown in Fig. 1. Failure to meet SRR may result in insufficient diffuse reflection energy for the laser seeker to identify the ground target.

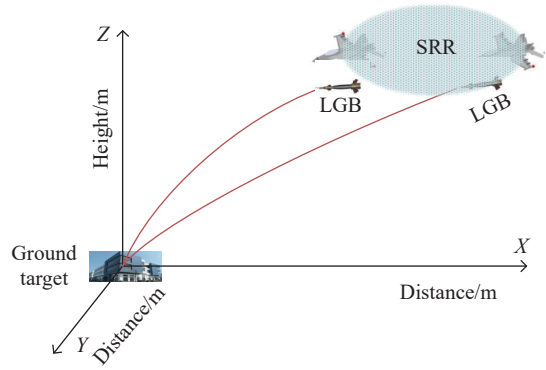

Fig. 1 Self-designation attack SRR

3. Laser-guided optical path model

The OGP is composed of two parts, one is the LDP irradiating the target and the other is the laser diffuse reflection energy from the target into the laser seeker.

3.1 Model of atmospheric transmittance

The aircraft acquires target information prior to the mission and proceeds to the designated airspace for detection, confirmation, and strike. Upon arrival at the designated airspace, the LDP emits a laser designation signal to illuminate the target and subsequently releases the bomb. The bomb's control component is unlocked two seconds after its release. The LGB guidance system becomes operational when the energy density received in the laser sight's field of view exceeds a specific threshold. To calculate the energy density value at the target point after decay, the atmospheric transmittance on the OGP needs to be determined. Given the initial energy of the LDP, the calculation of atmospheric transmittance enables the determination of energy density at the target point after decay.

In engineering calculations, the scattered extinction of the aerosol group can be approximated by applying the Mie scattering theory primarily [19]. The extinction coefficient is the sum of the scattering and absorption coefficients $\beta_e = \beta_s + \beta_a$. The relationship between atmospheric transmittance and the extinction coefficient [16] is expressed as follows:

$$\tau(\lambda) = \exp\left\{-\frac{\beta_e b R}{H}\left(1-\mathrm{e}^{-\frac{H}{b}}\right)\right\} \tag{1}$$

where λ is the wavelength of the laser, H is the vehicle's flight height in km, R is the oblique track length in km, b is the empirical distribution coefficient of the atmospheric haze over height. The extinction coefficient β_e is related to atmospheric visibility V_M as follows:

$$\beta_e = \frac{3.912}{V_M}\left(\frac{\lambda}{0.55}\right)^{0.585\sqrt[3]{V_M}}. \quad (2)$$

The flight and atmospheric parameters obtained from the flight tests help us calculate the atmospheric transmittance of the OGP.

3.2 Laser diffuse reflection model of the target

The LDP irradiates a target, forming a light spot. The irradiated spot generates a laser diffuse field in space. To determine the variation of the energy density received by the laser seeker with time, the value of the received energy can be calculated by using Lambert's cosine law.

Fig. 2 shows when the angle between the solid angle and surface normal vector is θ, and the angle between the LDP irradiation beam and surface normal vector is β. The relationship between the laser energy emitted by the target designator and the laser energy received by the laser seeker can be calculated as follows [20]:

$$P_\theta = \frac{\rho_\lambda P}{\pi}\cos\theta\cos\beta \mathrm{d}\Omega \mathrm{d}s \quad (3)$$

where Ω is the solid angle in the backscatter direction of the target, $\Omega = \pi D^2/4r^2$, s is the backscatter cross-section of the target, P is the effective energy of the laser spot on the target, ρ_λ is the laser diffuse reflectivity of the object, the spatial distribution of the diffuse equivalent energy of the target can be approximated as an ellipse with Gaussian energy distribution [21]. The backscatter cross-section of the target is expressed as

$$s = \frac{\pi R^2 a_l^2}{4}. \quad (4)$$

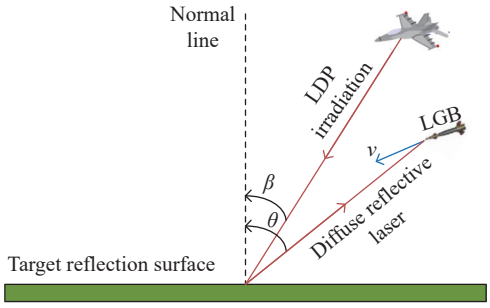

Fig. 2 LDP irradiation and laser diffuse reflection schematic

The formula shows that the backscatter characteristic of the target depends on the R, and the transmitter beam divergence angle a_l=0.5 mrad when a_l is very small, $a_l \to 0$, $\sin a_l \approx a_l$. The final energy density received by the LDP is obtained as

$$P_\theta = \tau_R(\lambda)\tau_r(\lambda)\rho_\lambda P_M \cdot \cos\theta\cos\beta\frac{D^2\pi R^2 a_l^2}{4r^2} \quad (5)$$

where $\tau_r(\lambda)$ is the atmospheric transmittance from the target to the laser seeker, $P = P_M \cdot \tau_R(\lambda)$, P_M is the pulsed laser beam energy emitted by the LDP, $\tau_R(\lambda)$ is the atmospheric transmittance from the LDP to the target. D is the receiver aperture diameter of the receiving optics, r is the distance from the laser seeker to the target.

4. Algorithm for calculating SRR

The SRR of the LGB is limited by multiple elements, such as the bomb's performance characteristics, initial release conditions, guidance law, atmospheric visibility, and target diffuse reflectance. The computational model of SRR is obtained through a comprehensive analysis of these parameters.

4.1 SRR longitudinal axis

When an aircraft is flying level at a specific speed, the ballistic plane can be regarded as coplanar with the target when the bomb's off-axis launch angle (between the target and the longitudinal axis of the aircraft) is minimal. To ensure that the munition strikes the target, only the roll attitude of the projectile needs to be adjusted until the laser seeker has received sufficient laser diffuse reflection energy. The following conditions must be met simultaneously:

(i) The angle between the laser seeker's optical axis and the target should be less than half of the field of view.

(ii) The energy density received by the laser seeker reaches a certain threshold.

(iii) The above two conditions need to be met along with the requirement of the guidance law.

According to the above rules, two boundary ballistics can be obtained. As shown in Fig. 3, when the LGB is at point A of ballistic trajectory 1, the angle between the target and the optical axis of the laser seeker is $\eta_m/2$, η_m is the field of view of the laser, the target is located at the edge of the field of view of the laser seeker. The energy density received by the laser seeker just reaches the threshold value at this point, and the LGB generates the guidance signal. While the LGB is at point B of ballistic trajectory 2, the angle between the target and the laser seeker is $-\eta_m/2$, and the received energy density is greater than the threshold value. The guidance signal is generated at this point as well. These two boundary ballistics simultaneously meet the requirements of the guidance law. As shown in Fig.3, the distance between the release points of the two boundary ballistics is SRR longitudinal axis L_l.

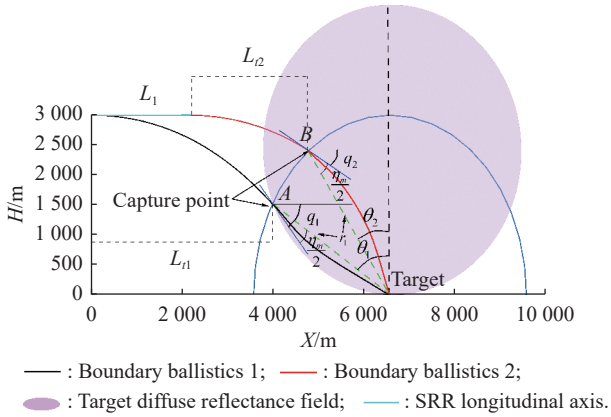

Fig. 3 Boundary ballistics and SRR longitudinal axis

In (5), cos β, cos θ, R, r,$\tau_R(\lambda)$, $\tau_r(\lambda)$are all time varying parameters, the relationship between $\tau_R(\lambda)$ and R has been derived from (1). Let P_θ be the threshold, after determining the various parameters as well as the expressions, the calculation is carried out using simulation software simulation modeling. While the three constraints are satisfied, the current level flight speed of the aircraft is v_0 and the distance between the aircraft and the target is R_1. The capture moment t_1 and maximum lock distance (MLD) r_1 become calculable values. Thus, the boundary ballistic 1 is obtained since the difference in ballistic inclination between the two boundary ballistic capture points is η_m and the distance to the target is also r_1, the capture moment t_2 of boundary ballistic 2 can be determined. Based on the ballistic model, the spatial locations of the initial release points of the two boundary ballistics can be calculated.

4.2 Solution of the SRR longitudinal axis

The initial conditions are shown in Table 1. The target's backscattered cross-section forms a diffuse field in space, which can be approximated as an ellipsoid [21]. The irradiance value on the surface of the ellipsoid is equal to the sensitivity threshold of the laser seeker. To determine the ballistic inclination, we use the relationship between ballistic inclination and time to compute the horizontal distance between the drop point and the capture point. The fitted curve of the ballistic inclination angle q and time t is as follow:

$$q = a + bt \tag{6}$$

where the values of a and b are determined by the different release speeds. The LGB can be considered a rigid body, and its trajectory before the arrival of the capture signal can be described [22] by the following equation:

$$\begin{cases} x = \dfrac{mv_0}{k}\left[1-\exp\left(-\dfrac{k}{m}t\right)\right] \\ y = \dfrac{mg}{k}t + \dfrac{m^2 g}{k^2}\left[\exp\left(-\dfrac{k}{m}t\right)-1\right] \end{cases} \tag{7}$$

where (x,y) is the spatial coordinate, k is the air resistance coefficient. The air resistance coefficient is related to the windward area of the bomb, air density, and the bomb's own coefficient of air resistance.

$$\theta_1 = \arctan\left(\frac{y_m - y_1}{x_m - x_1}\right) \tag{8}$$

where (x_m, y_m) is the coordinate of the target point, (x_1, y_1) is the coordinate of the capture point A, The analysis leads to the relationship between θ_1 and q_1 is

$$\begin{cases} q_1 + \theta_1 = 90^\circ + \dfrac{\eta_m}{2} \\ q_2 + \theta_2 = 90^\circ - \dfrac{\eta_m}{2} \end{cases}, \tag{9}$$

both θ_1 and q_1 are increasing functions with respect to time. The capture point A satisfies the condition $q_1 + \theta_1 = 90^\circ + \dfrac{\eta_m}{2}$, the numerical change curve can be obtained by simulation, the capture moment t_1 can be determined. Similarly, we can obtain θ_2, q_2, and t_2.

Table 1 Equipment parameters used in the simulation test.

Equipment	Parameters	Values
Aircraft	Flight height/km	3
	Speed/(m/s)	260
LDP	Energy/mJ	150
	Pulse width/ns	10-30
	Operating wavelength/μm	1.06
	Beam divergence angle/mrad	0.5
LGBs	Quality/ kg	500
	Aerodynamic area/m^2	0.111 6
	Equivalent aerodynamic length/m	0.4
	Max. field of view angle/(°)	30
	Roll, yaw, and pitch rotational inertia/(kg·m^2)	12.928 0 280
	Energy density threshold/(W/cm^2)	10^{-7}
	Optical aperture/mm	80
	Target diffuse reflectance/%	20

The horizontal distance from the capture points of the two boundary ballistics to the target are $r_1\sin\theta_1$,$r_1\sin\theta_2$. The horizontal distance traveled by the LGB before reaching the two capture points is

$$\begin{cases} L_{t1} = \dfrac{mv_0}{k}\left[1-\exp\left(-\dfrac{k}{m}t_1\right)\right] \\ L_{t2} = \dfrac{mv_0}{k}\left[1-\exp\left(-\dfrac{k}{m}t_2\right)\right] \end{cases}, \tag{10}$$

the SRR longitudinal axis L_l can be expressed as

$$L_l = r_1(\sin\theta_1 - \sin\theta_2) + (L_{t1} - L_{t2}) \tag{11}$$

where L_{t1} and L_{t2} are respectively the horizontal displacements before the capture moments of boundary ballistic 1 and boundary ballistic 2.

4.3 SRR transversal axis

SRR transversal axis depends on the capture time and the ability of the control system to correct the trajectory. Translate the boundary trajectory 1 in Fig. 3, towards the target direction obtain the boundary ballistic 1′, let θ at the moment of capture be equal to the ballistic inclination q, at this moment, the target point is on the extension line of the laser seeker optical axis. By simulation, we obtain the parameters θ_1', q_1', t_1' for the ballistic trajectory 1′. As shown in Fig. 4, translate the boundary ballistics 1′ to the boundary ballistics 3. Keeping the distance between the capture point and the target constant, let the yaw angle at the capture point C is $\eta_m/2$, and the target appears exactly at the edge of the laser seeker field of view. The transversal adjustment distance of the boundary ballistic 3 can be calculated. Similarly, we can get the boundary ballistic 4.

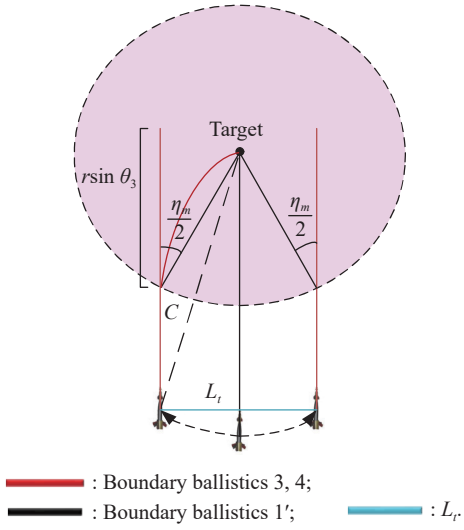

Fig. 4 Top view of ballistics

The distance between the boundary ballistic 3 and boundary ballistic 4 release points is SRR transversal axis and the expression is

$$L_t = 2r_1 \sin\theta_3 \sin\frac{\eta_m}{2} \tag{12}$$

where r_1 is still the distance from the capture point to the target, θ_3 is equal to θ_1'.

4.4 Guidance law constraint

In addition to determining the longitudinal and transverse axes, it is also necessary to consider the effect of the guidance method on the SRR. The weapon's aerodynamic layout and guidance system limit its ability to correct its ballistics. The LGB lacks a propulsion system, so ballistic corrections primarily come from the guidance system's control of the main lift surface to achieve the maximum lift-to-drag ratio and increase the weapon's range. Analysis of gliding ballistics by optimal lift-to-drag ratio is presented in [23]. First, the capture time versus horizontal velocity is obtained. The relationship between capture time and horizontal velocity is thus obtained.

$$u_1 = a\left[\frac{2}{\mathrm{e}^{\left(\frac{2a}{b}t_1 + 2aC_0\right)} + 1} - 1\right], \tag{13}$$

$$\begin{cases} a = \sqrt{g\delta} \\ b = K_{\mathrm{LD}}\delta \end{cases}, \tag{14}$$

$$C_0 = \left(\ln\frac{a+u_0}{a-u_0}\right)/2a, \tag{15}$$

where δ is the geocentric vector diameter, K_{LD} is lift-to-drag ratio, u_0 is the level initial velocity. Secondly, if the gliding initial velocity u_0 and final velocity u_e are known, the corresponding gliding range can be obtained

$$L_R = \frac{R_0 K_{\mathrm{LD}}}{2} \cdot \ln\frac{g\delta - u_e^2}{g\delta - u_0^2} \tag{16}$$

where R_0 is the radius of the Earth. Let $\dfrac{2g}{\beta K_{\mathrm{LD}}} = E$, β is the atmospheric density variation constant with height. The height of the weapon at the moment of capture is expressed as

$$H = \frac{Eb}{2}\ln\left(\mathrm{e}^{2aC_0 + 2ab^{-1}t} - 1\right) - \frac{E}{a}t + C_1, \tag{17}$$

$$C_1 = H_0 - \frac{Eb}{a^2}\ln\left(\mathrm{e}^{2aC_0} - 1\right), \tag{18}$$

where H_0 is the release height. Finally, we obtained all the parameters of the LGB's ballistic correction capability. Simulation calculations can determine whether the boundary ballistics meet the requirements of the guidance law. A lack of ballistic correction capability in the guided bomb usually occurs when the drop point is far from the target. If L_R is greater than the horizontal distance from the capture point to the target and the control time satisfies requirements simultaneously, then the

boundary ballistics are correctly selected. If L_R is less than the horizontal distance from the capture point to the target, then the initial release position must be shifted towards the target to satisfy $L_R = r_1 \sin\theta_1$ and ensure that control time meets requirements.

The SRR of the LGB depends on several factors. This paper uses simulation software to describe the numerical model and simulation steps (as show in Fig. 5). First, the ballistic model is determined, which includes calculating the guidance law based on the munition's muzzle velocity, altitude, mass, aerodynamic area, and maximum field-of-view angle. The output is the spatial coordinates of the LGB, clockwise velocity, angle of attack, distance to the target, ballistic inclination, and other data. Next, a target diffuse reflection model and a laser transmission model are constructed to characterize the energy distribution of the target in space after being irradiated by the laser pod versus the energy received by the laser seeker. The inputs are atmospheric transmittance, target diffuse reflectance, the minimum received energy threshold of the weapon laser seeker, and the transmit power of the pod light source. The output is the energy received by the laser seeker. Finally, simulation software simulation operations are used to find all initial placement points that satisfy the current initial conditions. The set of these spatial points is the expected result.

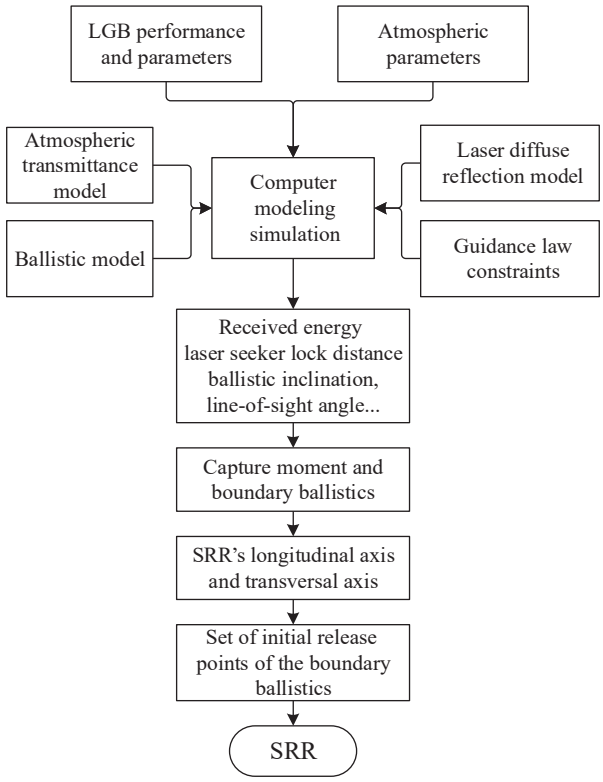

Fig. 5 Calculation flow of SRR

5. Simulation and result analysis

The semi-physical simulation test is based on the combination of the existing equipment. The aircraft, LDP and LGB parameters are shown in Table 1.

5.1 Laser seeker performance simulation analysis

The detection capability of the laser seeker is fixed. As such, atmospheric transmittance directly affects the capture moment, which in turn changes the SRR. The MLD of the laser seeker under different atmospheric visibility conditions can be deduced by using (1), (2), and (5).

From Fig.6, it is found that our MLD data are lower than the simulated data in [24] when visibility is greater than 5 km but less than 11 km. When visibility is greater than 11 km, our MLD data is higher than the simulation data in [24]. The difference may be due to variations in the extinction coefficient values or the different climate types selected [14].

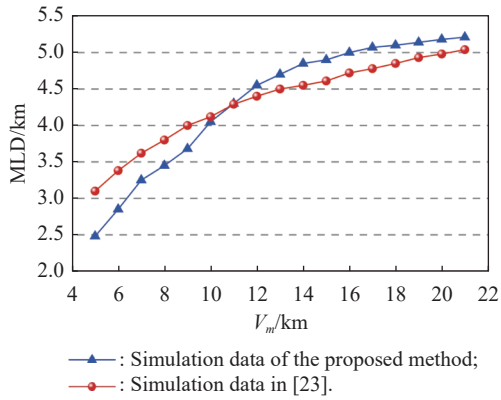

Fig. 6 MLD simulation test comparison chart

5.2 Simulation analysis of capture time

In this set of experiments, we analyzed various factors that influence energy variations on OGP. The first set of experiments examined the relationship between the illumination angle and atmospheric transmittance variation. The aircraft is positioned 7 km away from the target horizontally, with flight altitudes of 1 km, 2 km, 3 km, 5 km, and 8 km. The target's received energy density varied with changes in the LDP illumination angle and bomb-target distance. The relationship between the illumination angle and atmospheric transmittance is determined using (5). Curve fitting results are shown in Fig. 7. Simulation results demonstrated that atmospheric transmittance increases as the irradiation angle decreases. The illumination angle has a greater impact on atmospheric transmittance under low-altitude release conditions than under high-altitude release conditions, with transmittance peaking at an irradiation angle of 0°.

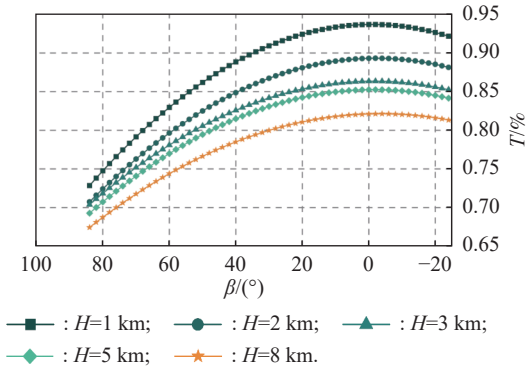

Fig. 7 The fitted curve of atmospheric transmittance with LDP illumination angle

The second set of experiments aimed to determine the energy density received by the laser seeker at different levels of atmospheric visibility. The release point altitude is 3 km and the horizontal distance between the release point and the target is 6.5 km. Simulation results showed that the generation time of the capture signal varied with visibility levels. As shown in Fig.8, at visibilities of 5 km, 8 km, 10 km, and 12 km, the corresponding capture times are 14.2 s, 12.8 s, 12.1 s, and 11.5 s, respectively. The earlier the control moment occurred, the more stable the control system became within a limited attitude control time, increasing the probability of impact. In low visibility conditions, capture time may be significantly delayed or may not meet the requirements of field of view or guidance law, resulting in a high probability of missing the target.

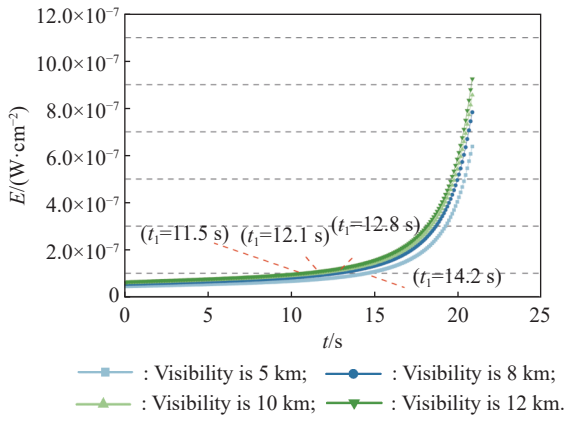

Fig. 8 Received irradiance curve with time

5.3 SRR simulation analysis

In the next set of tests, we calculated the SRR longitudinal axis for two visibility levels. The longitudinal distances between the initial positions of the two boundary ballistics and the target at the visibility of 7 km are 6 058 m and 3 695 m, making L_l=2 363 m (Fig. 9(a)), and at the visibility of 5 km are 5 754 m and 4 122 m, making L_l=1 632 m (Fig. 9(b)).

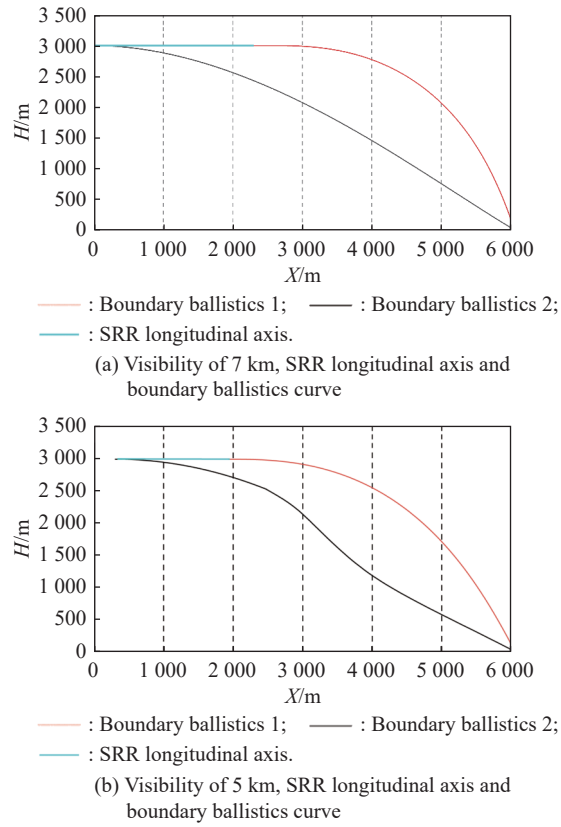

Fig. 9 Boundary ballistic curves at atmospheric visibility of 5 km and 7 km

We found that the SRR longitudinal axis is affected to a large extent as visibility decreased. Through simulation of 100 groups of visibility data, when visibility is greater than 5 km and less than 11 km, the average decrease of L_l is 73 m for every 0.2 km increase in visibility value, and the average decrease of L_l is 70 m for every 0.2 km increase in visibility when visibility is greater than 11 km.

The inclination curves of the two sets of boundary ballistics under different visibility conditions are shown in Fig. 10. Before the control signal is generated, the inclination angle of both boundary trajectories changes in the same trend. And after the control signal is generated, the inclination angle of the boundary ballistic 2 produces a significant change in magnitude, while the inclination angle of boundary ballistics 1 changes more gently. To guarantee a hit, the LGB that are farther from the target require sufficient glide distance. Fig. 10(a) shows at the visibility of 7 km, the capture moment for the two boundary ballistics respectively are 11.7 s and 9.1 s after release. Fig. 10(b) shows that at the visibility of 5 km, the

capture moment for the two boundary ballistics are 12.1 s and 9.5 s after release respectively. The further away from the target, the later the moment of capture will come. The lower the visibility is, the closer the distance between the two boundary ballistics.

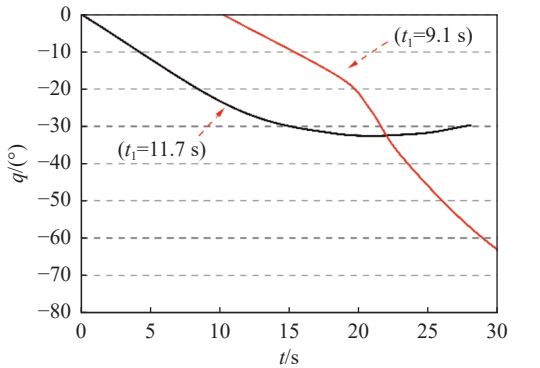

(a) Visibility 7 km, the inclination of the two boundary ballistics

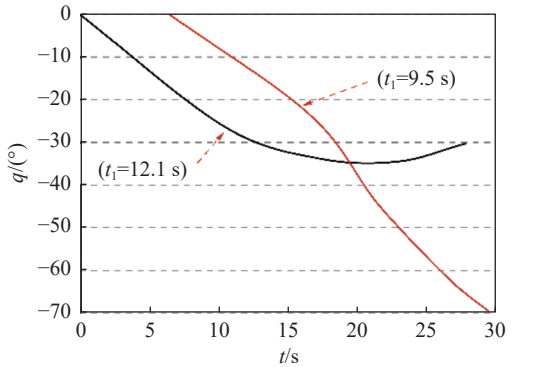

(b) Visibility 5 km, the inclination of the two boundary ballistics

Fig. 10 Boundary ballistic inclination curves of two groups under different visibility conditions.

The SRR at a level release speed of 260m/s for LGB is shown in Fig. 11. The spatial locations of SRRs with different flight speeds are also different, and the greater the speed the more distant the location relative to the target. The spatial extent of the SRR moves away from the target as the clockwise velocity of the release increases, and closer to the target as the release velocity decreases.

Fig. 12 shows the SRR profile at a flight altitude of 3 km and the level release speed of LGB is 260 m/s. Under the constraint of field of view and received energy threshold, the maximum allowable off-axis angle is also different under different visibility. After simulation V_m was taken as 5 km, 7 km and 10 km respectively, and the initial off-axis angle was not greater than 7.1°, 7.4°, and 7.9°. If the release speed increases, the SRR will move away from the target, and then the maximum allowed value of the off-axis angle at the release point will become smaller.

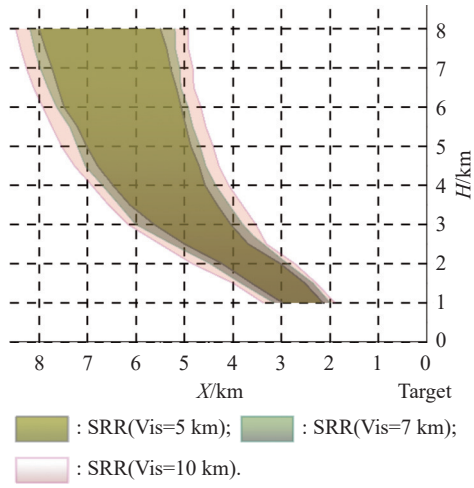

Fig. 11 SRRs at different atmospheric visibility

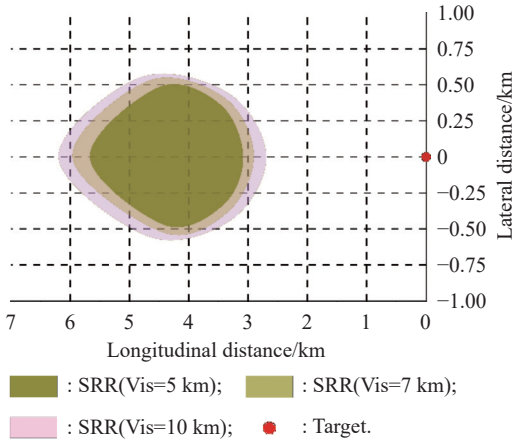

Fig. 12 SRR profile at 3 km altitude

5.4 Data validation

Flight test data is used to extract flight speed, altitude, launch off-axis angle, and release point coordinates. These parameters are then inputted into the computational model of SRR and compared with the actual placement point spatial locations in the data. If the result is a hit sample and within the SRR, the proposed method is deemed valid. If the sample is missing from the SRR, it is judged as a miss due to other reasons. Conversely, if the hit sample is not in the SRR, the method is considered invalid. However, if the miss sample is not in the SRR, the method is deemed valid. The hit results of the known samples are presented in Table 2, indicating that 91% of the samples are judged correctly, that is, the sum of the two percentages of SRR judgment accuracy, 81.5% and 9.5%. And 7.5% of the missing samples are due to other

factors. Additionally, 1.5% of the hit samples are not within the SRR, which may be attributed to parameter errors.

Table 2 Results of SRR determination of samples %

Ratio	Total sample	
	Hit samples	Miss samples
Within SRR	81.5	7.5
Outside SRR	1.5	9.5

With the previous data, we found that the hit samples in the SRR range and the missing samples outside the SRR range accounted for a larger percentage. This proves that the computational model of SRR is valid. Assuming that the release positions of all samples are within the SRR range, the hit probability can be improved more substantially. Therefore, we translated the initial release point coordinates of all samples outside the SRR range. The release point after translation satisfies the SRR model calculation results and improves the hit probability when applying the SRR model. As shown in Fig. 13, the probability of hitting all samples in the available statistical data is 83%. If all samples fit the SRR model calculation, the hit probability increases to 92.2%.

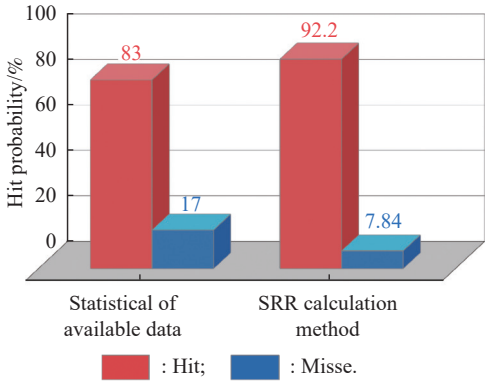

Fig. 13 Hit probability comparison graph

5.5 Error analysis

There is an inherent error in the method due to the measurement errors of atmospheric visibility. For urban targets, the visibility measurement error ranges from 3% to 26% [25]. In this paper, we used a median value of 10% for the calculation. Equations (1) and (2) show the relationship between transmittance and atmospheric visibility, while (5) shows the relationship between energy density and transmittance. The simulation experimental conditions are described in Subsection 5.2. With a visibility of 7 km, we obtained the relationship between changes in transmittance and capture time. Based on our simulation analysis of capture time and visibility, we derived the following function for the relationship between release point observation visibility and capture time:

$$t = 6.617\,7 \times 10^{-3} V_m^{\,2} - 0.443\,8 V_m + 15.986\,7. \quad (19)$$

If there is a 10% measurement error in V_m, then the capture moment will have a time error of 0.3 s. The distance error in the longitudinal direction is 78 m and in the transversal direction is 42 m. These errors account for 3.3% and 3.8% of the length of the SRR's longitudinal and transversal axis, respectively. When samples have different initial release conditions, their capture time versus visibility functions will also differ, leading to differences in computational error. The maximum computational error between the SRR's longitudinal and transversal axis through all data samples is 4.6%. We found that the lower visibility, the greater the error introduced. The mean value of the calculated error of SRR's longitudinal and transversal axis is 3.88%.

6. Conclusions

This paper argues that the ability of the laser seeker to receive diffuse reflection energy from the target is a prerequisite for the successful use of LGB to hit the target. To address this issue, a calculation method for quantifying the SRR of LGBs has been proposed. The calculation method is based on the ballistic model, laser propagation in the atmosphere model, laser diffuse reflection model, and ballistic model. The most significant findings of this study are as follows:

(i) Accurate calculation of the SRR of a LGB requires knowledge of several parameters, including the weapon's basic performance parameters, the carrier aircraft's flight altitude and speed, the state parameters at launch, atmospheric visibility, and guidance rate. Surprisingly, the initial release conditions of the aircraft are not the most significant factor affecting the SRR range. Instead, the main factor that reduces the SRR range significantly is atmospheric visibility.

(ii) The insights obtained from this study can assist in making appropriate adjustments to the relevant parameters based on the mission environment. To increase the probability of successful hits, it is recommended to minimize releases at the edge of the space release area or beyond. Moreover, using the SRR calculation method has been found to enhance the hit probability of LGB by 9.2%, and the method's validity and accuracy have been confirmed by flight test data.

(iii) The primary reason for error in the calculation of LGB'S SRR is the measurement error of atmospheric visibility. However, the calculation error is relatively small, at less than 4.6%.

To obtain a more accurate model, future work should consider both dive and loft release methods' SRR, given the complexity of the release conditions.

References

[1] KAUSHAL H, KADDOUM G. Applications of lasers for tactical military operations. IEEE Access, 2017, 5: 20736–20753.

[2] FAN J F, ZENG Z H. Study on the influence of battlefield environment on the combat effectiveness of laser-guided bombs. Mechatronics Information, 2015, 40(30): 170–171, 173.

[3] KOWALECZKO G, PIETRASZEK M, SŁONKIEWICZ Ł. Analysis of the impact of the target illumination time on the effectiveness of the flight trajectory correction system. Journal of KONBiN, 2019, 49(1): 229–253.

[4] ZHANG Q, LIU Y S. Simulation and contrast on three kinds of guidance law of guided bomb. Proc. of the International Conference on Machinery, Materials, Environment, Biotechnology and Computer, 2016, 3(45): 240−246.

[5] DAMLJANOVIC D, RISTIC S. Experimental investigation of aerodynamic characteristics of the laser guided bomb model. Vojnotehniki Glasnik, 2005(5): 406–417.

[6] HUANG Y, HE J, ZHOU M, et al. Researching integrated flight/fire control system of air-to-ground guided bombs. Computer Application, 2016, 34: 275–280. (in Chinese)

[7] CHEN S, GONG C, LI P. An approach to solve accessible region and release region of guided bomb. Systems Engineering and Electronics, 2001, 32(2): 28−30, 81.

[8] WANG W Z. Computation and simulation of a laser-guided bomb delivery domain. Aviation Computing Technology, 2009, 39(6): 53–57, 61.

[9] LEI K, LIN Z X. Research on guided bomb attack zone fitting algorithm. Electro-Optics and Control, 2013, 20(2): 85–88.

[10] LIU X C, GAO T C, LIU Z T. A study on the effect of atmospheric aerosols on laser transmission attenuation. Journal of Atmospheric and Environmental Optics, 2012, 7(3): 181–190.

[11] LV S, MA H, CHENG Y J, et al. Study on the impact of atmospheric scattering on laser-guided weapon countermeasures. Naval Electronics Engineering, 2014, 34(8): 162–165.

[12] LIU W C, QI L L, HE H J, et al. Numerical computational study of atmospheric transmission characteristics of 1.06 μm laser. Lasers and Infrared, 2011, 41(5): 520–524.

[13] GAVROUZOU M, HATZIANASTASSIOU N, GKIKAS A, et al. A global climatology of dust aerosols based on satellite data: spatial, seasonal and inter-annual patterns over the period 2005–2019. Remote Sensing, 2021, 13(3): 359.

[14] MA C L. Study on the influence of atmospheric transmission characteristics on laser detection performance. Xi'an: Xi'an University of Electronic Science and Technology, 2008.

[15] FAHEY T, ISLAM M, GARDI A, et al. Laser beam atmospheric propagation modelling for aerospace LIDAR applications. Atmosphere, 2021, 12(918). DOI: 10.3390/atmos-12070918.

[16] EVSIKOVA L G, GOREMYKIN Y A. Determining the atmospheric transmittance for laser wavelengths on an oblique track. Journal of Optical Technology, 2016, 83(8): 486–489.

[17] SUN C S, ZHANG X H, RAO J H, et al. A method for deploying diffuse reflector plate dummy targets in laser-guided deflection interference. Lasers and Infrared, 2013, 43(3): 252–255.

[18] PENG L J. Study of the radiation properties of target surface under laser irradiation. Wuhan: Huazhong University of Science and Technology, 2007.

[19] YE R J, YANG B Q, LI W S. Exploring the effect of atmospheric environment on the effectiveness of photoelectric interference. Photonics Applications, 2005(6): 24–27, 63.

[20] ZHANG W P, WU J H, HU X. Experimental method of optoelectronic countermeasure effect based on laser-guided head countermeasure data. Infrared and Laser Engineering, 2013, 42(3): 637–642.

[21] TONG Y, XIA M, YANG K C, et al. Target reflection feature extraction based on lidar intensity value. Laser Optoelectron Prog, 2018, 55(10): 102802.

[22] ALOMARI O, JARADAT E K, ALOQALI A D, et al. Solution for projectile motion in two dimensions with nonlinear air resistance using Laplace decomposition method. Journal of Mathematics and Computer Science, 2022, 12(1): 179–189.

[23] LI B J, WANG M H. Ballistic study of gliding segment of gliding long-range missile. Journal of Astronautics, 2009, 30(6): 2122–2126.

[24] YAO Y M, WEN Q S, LIU X J, et al. Research on the operational use performance of laser-guided bomb weapon system based on atmospheric visibility. Aerospace Weapons, 2017(3): 74–80.

[25] GUO H, ZHANG Z, JIANG L, et al. Angstrom exponent errors prevent accurate visibility measurement. Atmospheric Measurement Techniques, 2021, 14(3): 2441–2450.

Biographies

YANG Ping was born in 1985. He received his master's degree from Changchun University of Science and Technology. He is currently a Ph.D. student at the Air Force Early Warning Academy. His research interests are data mining and operational use of airborne guided weapons.
E-mail: vip_zzz@163.com

XIAO Bing was born in 1966. She received her Ph.D. degree from Huazhong University of Science and Technology. She is a lecturer at the Air Force Early Warning Academy. Her research interests are complex systems analysis and evaluation
E-mail: 494701394@qq.com

CHEN Xin was born in 1982. He received his Ph.D. degree from the National Defense University. He is an instructor at the Air Force Early Warning Academy. His research interests are cloud computing intelligent gaming and collaborative intelligence processing.
E-mail: cxin917@126.com

HAO Yuntao was born in 1976. He received his master's degree from the National Defense University. He is a sentor engieer at People's liberation Army Unit 93175. His research interests operational applications of tactical weapons, and are mission planning for air-to-ground guided weapons.
E-mail: vip_zzz1107@126.com